Biometals (2011) 24:279–289
DOI 10.1007/s10534-010-9394-1

Ferrous iron is found in mesenteric lymph bound to TIMP-2 following hemorrhage/resuscitation

James L. Atkins · Nikolai V. Gorbunov · Valerie Trabosh · Rachel Van Duyne · Fatah Kashanchi · Andrei M. Komarov

Received: 26 May 2010 / Accepted: 1 December 2010 / Published online: 13 January 2011

Abstract Extracellular iron has been implicated in the pathogenesis of post-injury organ failure. However, the source(s) and biochemical species of this iron have not been identified. Based upon evidence that distant organ injury results from an increase in intestinal permeability, we looked for ferrous iron in mesenteric lymph in anesthetized rats undergoing hemorrhage and fluid resuscitation (H/R). Ferrous iron increased in lymph from 4.7 nmol/mg of protein prior to hemorrhage to 86.6 nmol/mg during resuscitation. Utilizing immuno-spin trapping in protein fractions that were rich in iron, we tentatively indentified protein carrier(s) of ferrous iron by MALDI-TOF MS. One of the identified proteins was the metalloproteinase (MMP) inhibitor, TIMP-2. Antibody to TIMP-2 immunoprecipitated 74% of the ferrozine detectable iron in its protein fraction. TIMP-2 binds iron in vitro at pH 6.3, which is typical of conditions in the mesentery during hemorrhage, but it retains the ability to inhibit the metalloproteases MMP-2 and MMP-9. In summary, there is a large increase in extracellular ferrous iron in the gut in H/R demonstrating dysregulation of iron homeostasis. We have identified, for the first time, the binding of extracellular iron to TIMP-2.

Keywords Ferrous iron · TIMP-2 · Hemorrhage · Extracellular

J. L. Atkins (✉) · V. Trabosh
Closed Head Brain Injury Branch, Center for Military Psychiatry and Neuroscience, Walter Reed Army Institute of Research, 503 Robert Grant Ave., Silver Spring, MD 20910-7500, USA
e-mail: jim.atkins@us.army.mil

N. V. Gorbunov
The Henry M. Jackson Foundation for the Advancement of Military Medicine, Inc., Bethesda, MD 20889, USA

R. Van Duyne · F. Kashanchi
Department of Molecular and Microbiology, National Center for Biodefense and Infectious Diseases, George Mason University, Manassas, VA 20110, USA

R. Van Duyne · F. Kashanchi · A. M. Komarov
The George Washington University Medical Center, Washington, DC 20037, USA

Abbreviations

A&G bead	Protein A/G Sepharose beads
ALI	Acute lung injury
Brij-35	Ethoxylated dodecyl alcohol
Dcytb	Duodenal cytochrome B
DMPO	5,5-Dimethyl-1-pyrroline *N*-oxide
DTNB	5,5′-Dithiobis-(2-nitrobenzoic acid)
DTT	Dithiothreitol
DUSP-12	Dual specificity protein phosphatase 12
EDTA	Ethylenediaminetetraacetic acid
ELISA	Enzyme-linked immunosorbent assay

EPR	Electron paramagnetic resonance
HEPES	4-(2-Hydroxyethyl)-1-piperazineethanesulfonic acid
H/R	Hemorrhage/resuscitation
IP	Immunoprecipitation
MALDI-TOF MS	Matrix-assisted laser desorption/ionization time-of-flight mass spectrometry
MI/R	Mesenteric ischemia/reperfusion
MMP	Matrix metalloproteinase
NP-40	Nonyl phenoxypolyethoxylethanol
PBS	Phosphate buffered saline
PMSF	Phenylmethanesulfonylfluoride
SDS-PAGE	Sodium dodecyl sulfate polyacrylamide gel electrophoresis
TIMP-2	Tissue inhibitor of metalloproteinases-2
WLE	Whole lymph extract

Introduction

Trauma is the third leading cause of death in the United States resulting in over 170,000 deaths per year (AHRQ News and Numbers 2008) and it is the second most expensive medical condition, costing approximately $72 billion annually (Heron et al. 2009). Post-injury organ failure occurs in 7–30% of severely injured patients (Dewar et al. 2009) and it contributes significantly to both the morbidity and cost of post-injury care (Dewar et al. 2009; Ulvik et al. 2007).

Intestinal permeability increases following trauma and it has been implicated in the pathogenesis of multiorgan failure from many causes (Deitch et al. 2006; Lillehei 1957; Thomas and Balasubramanian 2004). The increase in permeability results in greater bacterial translocation and it is postulated to allow the permeation of serine proteases from the lumen of the intestine which contribute to the formation of pro-inflammatory mediators that can access the systemic circulation through mesenteric lymph (Penn et al. 2007). Mesenteric lymph in hemorrhage/resuscitation (H/R) activates neutrophils in vitro and H/R lymph is cytotoxic to endothelial cells in vitro (Deitch et al. 2006) while portal blood is not. Diversion of mesenteric lymph mitigates acute lung injury (ALI) after H/R (Deitch et al. 2006) and infusion of post-resuscitation mesenteric lymph into naïve rats causes ALI (Senthil et al. 2007). Exposure of cultured intestinal cells to iron increases monolayer permeability (Gonzalez et al. 1997), and systemic administration of the iron chelator desferroxamine in vivo decreases intestinal injury and limits bacterial translocation in H/R (Deitch et al. 1990), but addition of desferroxamine to mesenteric lymph in vitro does not prevent its cytotoxicity (Osband et al. 2003) suggesting that the intestine is the critical site of action of iron chelation in vivo.

Desferoxamine complexed with a large starch has limited cellular permeability (Paller and Hedlund 1994) but it is still able to mitigate hepatic dysfunction after H/R (Bauer et al. 1999; Rana et al. 2002; Rose et al. 2000) suggesting an important role for extracellular iron in this process. The biochemical species of this iron is unknown, but the possibility that ferrous iron could be involved was suggested by our findings that the ferroxidase activity of plasma ceruloplasmin was disrupted in hemorrhage (Atkins et al. 2005; Dubick et al. 2010). We have shown that the electron paramagnetic resonance signal of ceruloplasmin was decreased in the plasma of rats during hemorrhage (Atkins et al. 2005) and that the oxidase activity of plasma was decreased in combat casualties during the first 3 days after injury without a change in ceruloplasmin levels as determined by ELISA (Dubick et al. 2010).

Therefore, in the present study, we examined mesenteric lymph for the presence of ferrous iron in rats during H/R. We found a substantial increase in ferrozine detectable iron after resuscitation. Utilizing immuno-spin trapping (Gomez-Mejiba et al. 2009) we identified potential binding proteins for the iron and subsequently confirmed that antibody to one of these proteins (the metalloproteinase inhibitor, TIMP-2) immunoprecipitated a significant portion of the ferrozine detectable iron. TIMP-2 binds iron in vitro at a pH of 6.3 which approximates the pH in the mesentery during hemorrhage (Puyana et al. 2000). Iron binding does not affect the ability of TIMP-2 to inhibit the metalloprotease activity of MMP-2 or MMP-9 but the ability of TIMP-2 binding to prevent the deleterious actions of extracellular ferrous iron is still not known.

Methods

Materials

Ferrozine, ferrous sulfate, ammonium acetate, trichloroacetic acid, hydrogen peroxide and DMPO (5,5-dimethyl-1-pyrroline *N*-oxide) were purchased from Sigma-Aldrich (St. Louis, MO); Protein A&G beads were obtained from Calbiochem (San Diego, CA), anti-DMPO antibody was purchased from Alexis Biochemicals (San Diego, CA), Affinity-Pure polyclonal IgY antibody to DUSP-12 was acquired from GenWay Biotech, Inc. (San Diego, CA), ImmunoPure rabbit anti-chicken IgY (H + L) peroxidase conjugated was purchased from Thermo Scientific (Rockford, IL) and rabbit polyclonal antibody to TIMP-2 came from Abcam, Inc. (Cambridge, MA). All solutions were prepared using deionized Milli-Q water (Millipore, Bedford, MA).

Animal treatment

Animal handling and treatments were conducted in compliance with the Animal Welfare Act and other Federal statutes and regulations related to animals and experiments involving animals, and adhered to principles stated in the Guide to the Care and Use of Laboratory Animals, National Research Council. The facilities are fully accredited by the Association for Assessment and Accreditation of Laboratory Animal Care International.

The animal procedures have been previously described (Atkins et al. 2008). Briefly male Sprague–Dawley rats were anesthetized with ketamine (60 mg/kg i.p.) (NLS Animal Health, Owings Mills, MD) and anesthesia was maintained by supplemental injections of ketamine as required. The intestines were eviscerated beginning at the cecum and wrapped in saline moistened gauze. The post-nodal mesenteric lymphatic was cannulated adjacent to the take off of the mesenteric artery with silastic tubing (Dow Corning CAT # 508-002), and secured with cyanoacrylate. The intestines were then repositioned in the abdomen and the abdominal cavity was closed and lymph was collected on ice. Core temperatures were monitored and maintained at 37°C by a feedback control unit that monitors rectal temperature (Homeothermic Blanket, Harvard Apparatus, Holliston, MA). The animals received no heparin. The femoral artery was cannulated and used to monitor blood pressure and the femoral vein was cannulated and utilized for blood withdrawal and resuscitation.

After a control period of 20 min, the animals were hemorrhaged over 15 min to a mean arterial pressure of 40 mmHg. They were maintained at that pressure by intermittent blood withdrawal. Resuscitation was initiated when blood pressure could no longer be maintained by blood withdrawal and the mean arterial pressure began to fall below 40 mmHg (approximately 40 min). Thereafter the animals were resuscitated with a volume of lactated Ringers equal to three times the shed blood volume, infused over 1 h. No blood was reinfused into the rats. Lymph was collected on ice in three periods: (1) before hemorrhage (Control), (2) during hemorrhage, which includes the 15 min required to lower arterial pressure as well as the period when the animal was maintained at 40 mmHg (Hemorrhage), and (3) during resuscitation (Resuscitation). The lymph was centrifuged to remove formed elements and frozen in liquid nitrogen until subsequent analysis.

Analysis of lymph

Lymph was analyzed for ferrous iron by the ferrozine assay. Lymph was exposed to hydrogen peroxide with the spin trap DMPO and examined by electron paramagnetic resonance for evidence of hydroxyl radicals. Having demonstrated that the ferrous iron was reactive, the lymph was fractionated by size-exclusion chromatography. The fractions with significant ferrous iron content were exposed to hydrogen peroxide and DMPO and the DMPO-adducts were immunoprecipitated using anti-DMPO antibody cross-linked to protein A&G beads. The protein immunoprecipitates were used for Western blot and MALDI-TOF MS analysis of DMPO labeled proteins from lymph. Tentative identification of these proteins was obtained using peptide mass fingerprinting analysis software. Antibodies for two of the identified proteins (DUSP-12 and TIMP-2) were used to immunoprecipitate proteins and the decrement in ferrozine detectable iron was measured. (The details of these methods follow.)

Ferrozine assay

Iron(II) levels were determined using the colorimetric reagent ferrozine (Carter 1971; Stookey 1970) as

Table 1 Fractions from the size exclusion chromatography that contained high levels of ferrous iron and tentative identification of proteins in these fractions that were isolated by immuno-spin trapping and IP

Fraction	Spot	Molecular mass (kDa)	Fe(II) concentration (μM)	Tentative proteins
13	4	~1000–2000	1.8	Protein kinase A, FMS-related tyrosine kinase, TIMP-2
14	5, 7	~1000–2000	1.0	Olfactory receptor, phospholipid hydroperoxide glutathione peroxidase, mitochondrial precursor, carbohydrate sulfotransferase 7
38	6	~150–200	2.3	DUSP-12

This table presents fractions 13, 14 and 38 from the size exclusion chromatography that have the highest concentration of iron. Proteins within these fractions were isolated by immuno-spin trapping with DMPO and IP and tentatively identified by MALDI-TOF MS

modified by Alford et al. (1991). Proteins were precipitated with TCA. All iron in the Fe(II) form was complexed with ferrozine, and measured at 562 nm using a Beckman DU 650 spectrometer.

EPR spectroscopy and spin trapping with DMPO

All EPR measurements were done using a Bruker ER-200 X-band EPR spectrometer. Samples (50 μl) in capillary tubes (0.5 mm i.d.) were examined at room temperature. Formation of DMPO adducts was detected in the lymph fluid (without additional Fe) using 120 mM DMPO and 44 mM of hydrogen peroxide. Instrumental conditions were microwave frequency 9.71 GHz; center field 3472 G; scan rate 100 G/200 s; modulation amplitude 1.25 G; time constant 0.5 s; microwave power, 10 mW.

Size-exclusion chromatography

Whole lymph fluid was fractionated on a Superose 6 HR 10/30 column (Amersham Biosciences, Piscataway, NJ) in Buffer D (20 mM HEPES (pH 7.9), 50 mM KCl, 0.2 mM EDTA, 0.5 mM PMSF, 50 mM DTT and 20% Glycerol). Flow-through was collected at 0.5 ml for 50 fractions. Fractions were analyzed for iron by ferrozine assay. The chromatography of whole lymph was performed in non-denaturing conditions and therefore molecular masses for these fractions (Table 1) may be higher than molecular masses of the specific proteins identified in these fractions by MALDI-TOF and database analysis (due to protein aggregation or formation of complexes).

DMPO labeling and immunoprecipitation of DMPO-labeled proteins

Fractions that were rich in iron were reacted with 120 mM DMPO and 0.44 M H_2O_2 for 2 h at room temperature. One hundred microliters of DMPO-labeled iron rich fractions were incubated while rotating overnight at 4°C with 100 μl anti-DMPO cross-linked beads (see below). A negative control included 100 μl of rat lymph fraction incubated with 100 μl of anti-IgG cross-linked beads. Beads were washed twice with TNE_{300} + 0.1% NP-40 followed by TNE_{50} + NP-40. Elution of bound proteins was performed by heating the beads at 56°C for 20 min in 100 μl of 1.0 M glycine. Solutions were centrifuged and supernatants neutralized using 6 μl 1.0 N NaOH. Laemmli buffer (2×) was added, samples were heated for 3 min at 95°C, and loaded for SDS-PAGE analysis.

MALDI-TOF analysis

Individual protein spots were excised from Coomassie-stained gel using a clean razor blade, washed, trypsinized, and eluted. Trypsin-digested sample solutions were further desalted and concentrated with C18 ZipTips. Samples were mixed with equal volumes (1 μl) of the matrix solution, applied to the MALDI sample plate, and introduced into the mass spectrometer after drying. Mass spectra were recorded in the reflectron mode of a MALDI-TOF mass spectrometer (Shimadzu Axima CFRplus).

Database analysis

Peak analysis was performed using Mascot Distiller and peak lists were corrected by subtracting negative

control and matrix background peaks. Proteins were identified and compared using the peptide mass fingerprinting analysis software ProFound and Mascot. The NCBInr and the Swiss-Prot database were used for the searches with several passes of searching with different limitations for each spot. In general, all spots were searched with no modifications and no-limitation for using the "Rattus" taxonomy option. The best match for each spot was considered with highest coverage rate, more matched peptides, highest score without limitation protein mass, and selection from both databases. One missed cleavage by trypsin and lowest mass tolerance, i.e. 1.0 Da were considered for most of the proteins. We consistently used various multiple parameters such as low missed cleavages, low ppm, and others in our searches to obtain more reliably matched proteins.

Anti-DMPO, Anti-DUSP-12 and anti-TIMP-2 antibody cross-linking

One hundred μl of specific antibody to DUSP-12, DMPO or TIMP-2 (see Materials above) was incubated rotating overnight at 4°C with 200 μl of 30% Protein A&G beads slurry (Calbiochem IP05). Antibodies were cross-linked to the beads by the addition of 200 mmol/l triethanolamine in PBS to which 20 mmol/l dimethyl pimelimidate was added directly before use. Beads were rotated for 30 min and washed with 200 mmol/l triethanolamine in PBS. Addition of triethanolamine followed by wash was repeated and the reactive groups were quenched by the addition of 50 mmol/l ethanolamine in PBS, incubated for 60 min. The beads were incubated twice for 20 min each at 56°C with 1.0 M glycine–HCl. Beads were stored at 4°C in PBS with 0.2 ml/l Tween-20 and 0.2 g/l sodium azide until use. Protocol was repeated with 10 μl anti-IgG (mouse) in 40 μl beads as a control.

Immunoprecipitation of DUSP-12 and TIMP-2

100 μl of rat lymph fraction 13 or 38 was incubated rotating overnight at 4°C with 100 μl anti-DUSP-12 or anti-TIMP-2 cross-linked beads. Negative control included 100 μl of rat lymph fraction incubated with 100 μl of anti-IgG cross-linked beads. The samples were centrifuged and the supernatant was analyzed for iron with the ferrozine assay.

In vitro iron-loading of TIMP-2

Recombinant TIMP-2 was purchased from R&D Systems (Minneapolis, MN) and reconstituted according to manufacturer's suggestions with TCNB buffer (50 mM Tris, 10 mM $CaCl_2$, 150 mM NaCl, and 0.05% Brij-35, pH 7.5). Reconstituted TIMP-2 was brought to a concentration of 96 nM in buffer containing 200 mM HEPES, 100 mM NaCl, and 10 μM sodium dithionite, pH 7.4 in the presence or absence of a tenfold excess of iron (960 nM ammonium ferrous sulfate). Samples were titrated down to pH 6.3 with the drop-wise addition of concentrated HCl and incubated for 1 h at room temperature. Control samples were kept at equal concentrations by the addition of water. Following the 1 h incubation, the pH of the samples was restored back to pH 7.4 with the addition of concentrated NaOH, and incubated for an additional 1.5 h. Thirty minutes after the addition of NaOH (water in controls), the UV–VIS spectra was obtained using a Nanodrop spectrophotometer (Wilmington, DE).

In vitro determination of ability of TIMP-2 and TIMP-2 (Fe(II)) to inhibit MPP-2 and MMP-9

The inhibitory effect of TIMP-2 on MMP-2 and MMP-9 was determined using a colorimetric assay from Enzo Life Sciences (Plymouth Meeting, PA) according to the manufacturer's protocol. Briefly, MMP-2 or MMP-9 enzyme was incubated in the presence of TIMP-2/Fe or TIMP-2 (5 nM) for 30 min at 37°C in 50 mM HEPES, 10 mM $CaCl_2$, 0.05% Brij-35, 1 mM DTNB at pH 7.5. Following the incubation, a thiopeptide, chromagenic substrate specific for MMP-2 or MMP-9 was added to the reaction mixture and the subsequent activity of MMP-2 or MMP-9 was monitored over time by measuring the absorbance at 412 nm.

Results

Detection of TIMP-2 (Fe(II)) in the lymph fluid

In preliminary experiments, we examined post-resuscitation mesenteric lymph with low temperature electron paramagnetic resonance. We found little change in the high-field and low field ferric signal

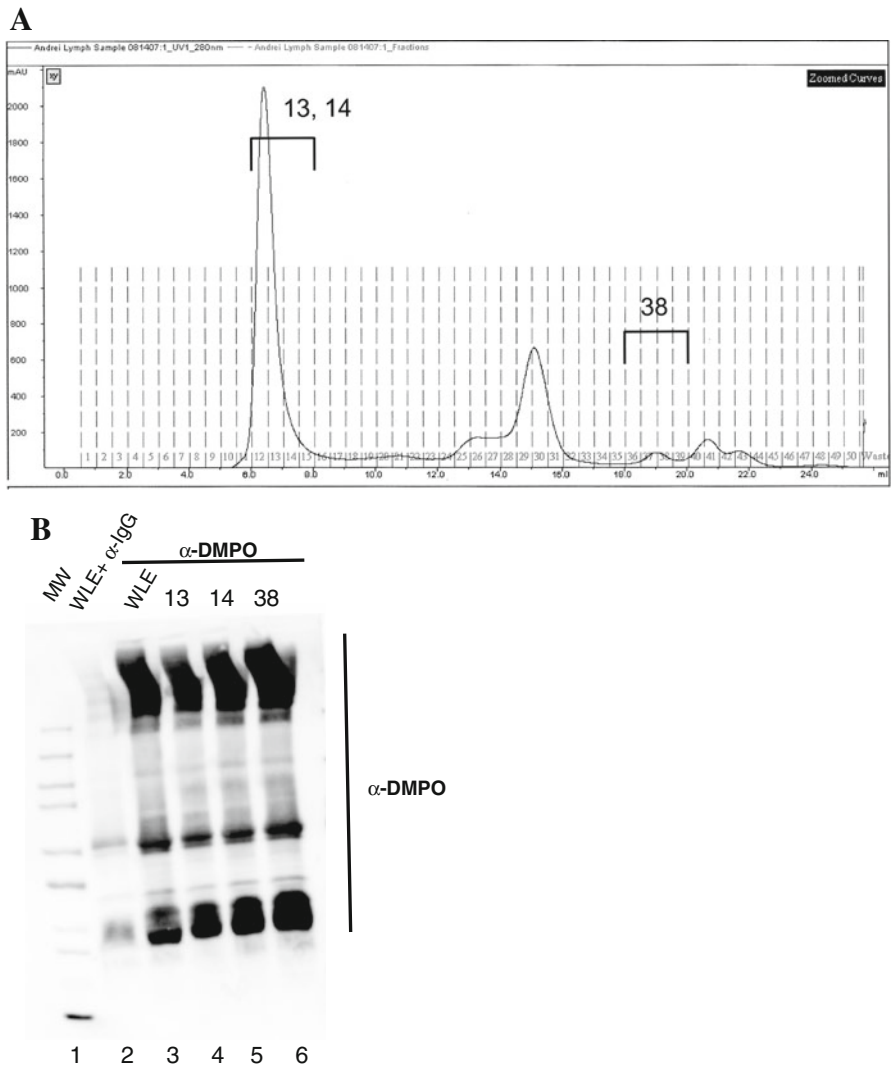

Fig. 1 Fractionation and IP of mesenteric lymph. **a** Mesenteric lymph was collected following H/R and subjected to fractionation on a Superose 6 HR 10/30 Column. The relative absorbance in the UV range (280 nm) is shown for each of 50 fractions. **b** IPs of DMPO from DMPO-containing FPLC fractionated samples 13, 14, and 38 were performed followed by western blot analysis for DMPO. *Lane 1* is the molecular weight marker, *lane 2* represents WLE IPed with α-IgG as a negative control, and *lane 3* represents WLE IPed with α-DMPO. *Lanes 4–6* represent fractions 13, 14, and 38 respectively, IPed with α-DMPO. Note, that the extracts loaded in *lane 3* are of a higher concentration than that of *lanes 4–6*

when comparing pre-hemorrhage to post-resuscitation, indicating little change in ferric iron in lymph. We also found no detectable signal for ceruloplasmin in post-resuscitation lymph (data not shown). The later finding suggests that the ferroxidase activity of ceruloplasmin was absent in lymph. Post-resuscitation lymph also contained Dcytb, a ferrireductase as detected by western blotting (data not shown). The lack of normal ferroxidase activity and secretion of Dcytb along with the oxidative stress induced by reperfusion could favor the formation and persistence of ferrous iron. This possibility was explored using the ferrozine assay. There was a substantial amount of ferrous iron in mesenteric lymph that increased during resuscitation (Table 2). Boiling post-resuscitation lymph with H_2O_2 resulted in the appearance of a high-field signal on electron paramagnetic resonance that is consistent with the conversion of ferrous iron to ferric iron. The concentration was similar to the concentration of ferrous iron detected by ferrozine (data not shown). As previously shown, the protein concentration falls in lymph during resuscitation from 27 to 11 μg/μl while flow rates increase from 0.02 ml/min during hemorrhage to 0.04 ml/min during resuscitation (Atkins et al. 2008). This would indicate that mass flow of ferrous iron increased during resuscitation. Reaction of the lymph with hydrogen peroxide and the spin trap DMPO resulted in the formation of hydroxyl DMPO-OH adducts (1:2:2:1 quartet with

Table 2 Range of Fe(II) per protein ratio in the mesenteric lymph of rats subjected to hemorrhage and subsequent fluid resuscitation

Treatment	nmol Fe/mg protein
Control	4.7 ± 0.9 ($n = 3$)
Hemorrhage	10.3 ± 2.8 ($n = 4$)
Resuscitation	86.6 ± 26.5 ($n = 5$)[a]

Iron levels in lymph samples were quantified with the ferrozine assay under Normal, Hemorrhage and Resuscitation conditions and were seen to be significantly higher following resuscitation. All results are expressed as mean ± SE of 3–5 experiments. Statistical differences between the groups were determined using a one-way ANOVA. Subsequently the Tukey test was used to test all pair wise comparisons between the groups. Analysis was performed using statistical analysis software SigmaStat for Windows (Version 3.01A). Statistical significance level was set at $P < 0.05$

Table 3 Ferrous iron concentration in chromatography fractions before and after immuno-precipitation with antibodies to TIMP-2 and DUSP-12

Fraction	Treatment	Fe(II) concentration (μM)
13	Anti-IgG	3.1
13	Anti-TIMP-2	0.8
38	Anti-IgG	3.9
38	Anti-DUSP-12	3.9

Fractions 13 and 38 were immunoprecipitated with anti-IgG or TIMP-2 and DUSP-12 and the resultant levels of iron in the immunodepleted supernatants were quantified with the ferrozine assay. Immunodepletion of TIMP-2 lowered the iron concentration by approximately fourfold when compared to the IgG control. Depletion of DUSP-12 failed to decrease the iron concentration of the lymph samples suggesting that DUSP-12 is not capable of binding iron while TIMP-2 has that ability

hyperfine coupling constant: $a^N = a^H_\beta = 14.9$ G) (data not shown).

In order to identify specific DMPO-tagged proteins within the lymph, we performed size exclusion chromatography to identify iron rich fractions. The spectrum in Fig. 1a indicates the elution profile of single proteins and protein complexes within the lymph sample as measured by UV absorbance at 280 nm. Three fractions carried substantial ferrous iron: fractions 13, 14, and 38 (Table 1). In order to confirm that these fractions contain DMPO-tagged proteins, immunoprecipitations (IPs) followed by Western blots of whole lymph, and fractions 13, 14, and 38 were performed (Fig. 1b). The large bands at approximately 50 and 20 kDa in both the α-IgG and the α-DMPO lanes represent the heavy and light chain of the antibody used to IP the proteins as detected nonspecifically by the probing antibody. The absence of unique protein bands in lane 2 and the presence of bands in lanes 3–6 confirm that these fractions do contain DMPO-tagged proteins. In order to specifically identify these proteins, whole lymph, and the three fractions of interest were IPed with α-DMPO and run on a 4–20% SDS-PAGE gel. Unique protein bands were excised, trypsin-digested, and subjected to MALDI-TOF analysis. Protein mass fingerprinting analysis of the unique peptide peaks allowed the tentative identification of proteins, as shown in Table 1. Of note, TIMP-2 had also been identified in preliminary analysis of unfractionated lymph. Immunoprecipitation with antibodies to DUSP-12 did not remove iron, while IP with TIMP-2 removed most of the iron in fraction 13 (Table 3). The results show that 74% of Fe(II) present in lymph fraction 13 precipitates with TIMP-2.

In vitro binding of iron to TIMP-2

In preliminary experiments TIMP-2 was exposed to iron at pH 7.4, but there was no significant change in the UV–Vis spectrum (data not shown). Because the pH of the intestine falls to 6.3 during hemorrhage (Puyana et al. 2000), we conjectured that the fall in pH in the mesentery during hemorrhage may unveil a metal binding site on TIMP-2 that is not normally seen at pH 7.4. Consistent with this assumption, in preliminary experiments we detected the appearance of an absorbance band at 230 nm when TIMP-2 was exposed to ferric iron and ascorbate and titrated down to pH 6.3 and then returned to pH 7.4 (data not shown). We went on to examine this in more detail in the absence of ascorbate but in the presence of dithionite as described in the methods. Absorbance spectra of the compositions are presented in Fig. 2a. The UV spectra represent unresolved lines comprised of several bands (Fig. 2a). Therefore, we generated the second derivative of UV–VIS spectra (Fig. 2b) to demonstrate effect of TIMP-2 in Iron–TIMP-2 composition in the presence of transitional changes of pH in the range of pathophysiological conditions. That effect appeared as a shift of maximum of Iron–TIMP-2 spectral band to longer (red) wavelength. The findings are consistent with the formation of a TIMP-2 iron complex.

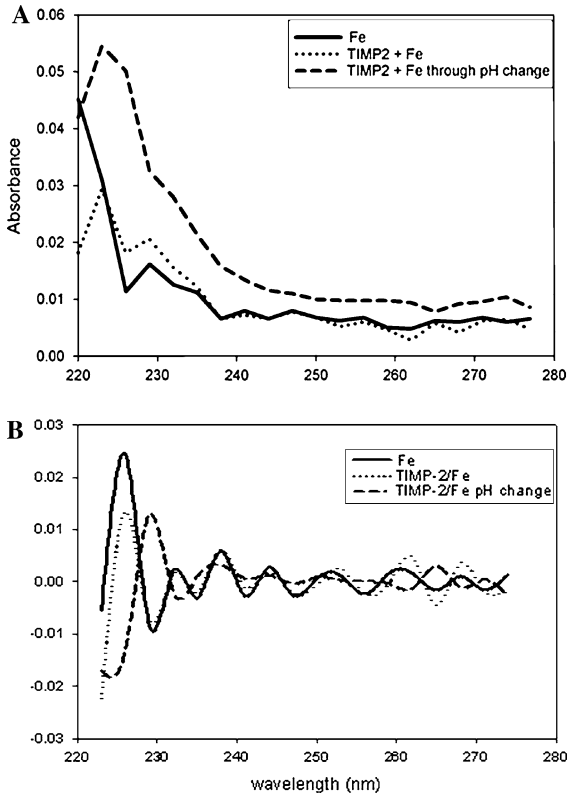

Fig. 2 In vitro binding of iron to TIMP-2. TIMP-2 (96 nM) was incubated in the presence or absence of 960 nM ammonium ferrous sulfate while subjected to a pH titration or remaining constant at pH 7.4. Final conditions were the same for all samples and absorbance spectra were obtained 30 min after resuming physiological pH 7.4 (**a**). Titration of TIMP-2 through a pH change resulted in the appearance of an absorbance band at approximately 230 nm. **b** Second derivatives of absorbance were plotted against wavelength (nm) to emphasize the precise position of the TIMP-2/Fe(II) peak

In vitro determination of ability of TIMP-2 and TIMP-2 (Fe(II)) to inhibit MPP-2 and MMP-9

TIMP-2 is a strong inhibitor of MMP-2 and MMP-9 and this was unchanged after binding iron (data not shown).

Discussion

The "gut" has been named the "engine of multiorgan failure" and an increase in intestinal permeability is believed to drive this process either through the generation of pro-inflammatory mediators within the enterocyte (Jordan et al. 2008; Penn et al. 2007) or by disrupting the intricate balance between the intestinal contents and the gut-associated lymphoid tissue (GALT) (Clark and Coopersmith 2007). The role of dysregulated iron handling in the intestinal injury is supported by the findings that the iron chelator desferoxamine limits intestinal injury in H/R (Deitch et al. 1990) and following mesenteric ischemia/reperfusion (MI/R) (Lelli Jr et al. 1993). The results of the present study provide further evidence of dysregulated iron handling, demonstrating a substantial increase in ferrous iron in mesenteric lymph after H/R. The iron dysregulation in H/R may involve other tissues besides the intestine as a recent study by Kozlov et al. (2010) has shown increased free iron in the liver in trauma-hemorrhage.

We have shown that the ferrous iron in mesenteric lymph is bound to the metalloprotease inhibitor TIMP-2, raising the possibility that this binding could contribute to intestinal hyperpermeability through a loss of inhibitory activity and a resultant increase in net metalloprotease activity. It is known that MMP-9 activity is increased in MI/R (Rosario et al. 2004) and metalloprotease activation is involved in the oxidant-induced increase in permeability of intestinal Caco-2 cells in culture (Forsyth et al. 2007). In order to test this hypothesis we measured the ability of TIMP-2 (Fe(II)) to inhibit MMP-2 and MMP-9. The inhibitory action of TIMP-2 was unchanged, indicating that the binding of ferrous iron to TIMP-2 does not alter the function of the inhibitory N-terminus region of the protein. However, TIMP-2 can also increase MMP activity through the activation of Pro-MMP-2 which requires the binding of the C-terminus domain of TIMP-2 forming a trimolecular complex at the cell surface (English et al. 2006). We have not yet examined if iron binding to TIMP-2 can accelerate Pro-MMP-2 activation and thus increase intestinal permeability.

Evidence would suggest that the local increase in extracellular ferrous iron may be a general phenomenon of reperfusion injuries. Oxidative stress causes an increase in intracellular labile iron which can escape from the cell (Huang et al. 2001; Iwatsuki et al. 2008). In I/R injury to the lung some of the released iron was reactive with bleomicin, which is consistent with the presence of ferrous iron (Huang et al. 2001). Iron can also be released from the cell while bound to ferritin. This is potentially a mechanism of targeted delivery to distant organs (Bresgen

et al. 2010; Fisher et al. 2007). It is unknown if TIMP-2 bound iron can also contribute to iron uptake in distant organs. Extracellular ferrous iron may participate in paracrine signaling. An extracellular binding site for ferrous iron has recently been identified for insulin-like growth factor binding protein-3 and binding of ferrous iron to this site influences signaling (Singh et al. 2004). It is currently unknown if the binding of iron influences the TIMP-2 signaling pathways that are independent of its metalloprotease inhibitory activity (Stetler-Stevenson 2008).

TIMP-2 secretion increases during reoxygenation (Cavdar et al. 2010) and our current working hypothesis is that this is a general protective mechanism, both by inhibiting the activity of MMPs and binding reactive iron. Unbound extracellular ferrous iron could be deleterious in many ways. It could provide an essential nutrient for proliferation of bacteria (Bullen et al. 2006; Eaton 2002) that have translocated across the intestinal wall during H/R. It can participate in the Haber–Weiss reaction resulting in oxidative injury and the Fenton reaction which results in the formation of hydroxyl radicals and facilitates protein nitration (Thomas et al. 2002). Protein nitration occurs in the intestine during H/R as evidenced by heavy staining with anti-nitrotyrosine following H/R (Liaudet et al. 2000). Ferrous iron has also been shown to be involved in complement activation in MI/R as desferoxamine limits complement activation (Turnage et al. 1994). Complement activation is an important mediator of both local and distant tissue injury in MI/R (Stahl et al. 2003). It will be important to determine if the binding of iron to TIMP-2 prevents these deleterious actions.

In summary we have demonstrated that mesenteric lymph contains a significant amount of ferrous iron after resuscitation from systemic hemorrhage. We have also identified a new protein carrier of ferrous iron, TIMP-2, which binds iron under the conditions existent during mesenteric hypoperfusion/ischemia. We postulate, that iron binding may limit the increase in intestinal permeability and thus protect from distant organ injury.

Acknowledgments We wish to thank Dr. Edwin A. Deitch for advice on the technique for the cannulation of mesenteric lymphatics and Sara Smith for her excellent technical assistance. This work was supported by the Department of the Army Peer Reviewed Medical Research Program, no. PR033201 (Atkins).

Disclaimer The views, opinions, and/or findings contained herein are those of the authors and should not be construed as an official position, policy or decision of the Department of the Army or Uniformed Services University of the Health Sciences.

References

AHRQ News and Numbers (2008) Big money: cost of 10 most expensive health conditions near $500 billion. http://www.ahrq.gov/news/nn/nn012308.htm. Accessed 26 May 2010

Alford CE, King TE Jr, Campbell PA (1991) Role of transferrin, transferrin receptors, and iron in macrophage listericidal activity. J Exp Med 174:459–466

Atkins JL, Day BW, Handrigan MT, Zhang Z, Pamnani MB, Gorbunov NV (2005) Brisk production of nitric oxide and associated formation of *S*-nitrosothiols in early hemorrhage. J Appl Physiol 100(4):1267–1277. doi:10.1152/japplphysiol.01059.20058750-7587/06

Atkins JL, Hammamieh R, Jett M, Gorbunov NV, Asher LV, Kiang JG (2008) Alpha-defensin-like product and asymmetric dimethylarginine increase in mesenteric lymph after hemorrhage in anesthetized rat. Shock 30:411–416. doi:10.1097/SHK.0b013e31816a71cb

Bauer C, Walcher F, Holanda M, Mertzlufft F, Larsen R, Marzi I (1999) Antioxidative resuscitation solution prevents leukocyte adhesion in the liver after hemorrhagic shock. J Trauma 46:886–893

Bresgen N, Jaksch H, Lacher H, Ohlenschlager I, Uchida K, Eckl PM (2010) Iron-mediated oxidative stress plays an essential role in ferritin-induced cell death. Free Radic Biol Med 48:1347–1357. doi:10.1016/j.freeradbiomed.2010.02.019

Bullen JJ, Rogers HJ, Spalding PB, Ward CG (2006) Natural resistance, iron and infection: a challenge for clinical medicine. J Med Microbiol 55:251–258. doi:10.1099/jmm.0.46386-0

Carter P (1971) Spectrophotometric determination of serum iron at the submicrogram level with a new reagent (ferrozine). Anal Biochem 40:450–458

Cavdar Z, Oktay G, Egrilmez MY, Genc S, Genc K, Altun Z, Islekel H, Guner G (2010) In vitro reoxygenation following hypoxia increases MMP-2 and TIMP-2 secretion by human umbilical vein endothelial cells. Acta Biochim Pol 57(1):69–73

Clark JA, Coopersmith CM (2007) Intestinal crosstalk: a new paradigm for understanding the gut as the "motor" of critical illness. Shock 28:384–393. doi:10.1097/shk.0b013e31805569df

Deitch EA, Bridges W, Berg R, Specian RD, Granger DN (1990) Hemorrhagic shock-induced bacterial translocation: the role of neutrophils and hydroxyl radicals. J Trauma 30:942–951

Deitch EA, Xu D, Kaise VL (2006) Role of the gut in the development of injury- and shock induced SIRS and MODS: the gut-lymph hypothesis, a review. Front Biosci 11:520–528. doi:10.2741/1816

Dewar D, Moore FA, Moore EE, Balogh Z (2009) Postinjury multiple organ failure. Injury 40:912–918. doi:10.1016/j.injury.2009.05.024

Dubick MA, Park MS, Barr JB, Atkins JL (2010) Ceruloplasmin oxidase (CPO) activity in plasma from burn and non-burn trauma patients. Inflamm Res 59:S125

Eaton JW (2002) Bugs, guts, and iron. Shock 18:483–484

English JL, Kassiri Z, Koskivirta I, Atkinson SJ, DiGrappa M, Soloway PD, Nagase H, Vuorio E, Murphy G, Khokha R (2006) Individual Timp deficiencies differentially impact pro-MMP-2 activation. J Biol Chem 281:10337–10346. doi:10.1074/jbc.M512009200

Fisher J, Devraj K, Ingram J, Slagle-Webb B, Madhankumar AB, Liu X, Klinger M, Simpson IA, Connor JR (2007) Ferritin: a novel mechanism for delivery of iron to the brain and other organs. Am J Physiol Cell Physiol 293:C641–C649. doi:10.1152/ajpcell.00599.2006

Forsyth CB, Banan A, Farhadi A, Fields JZ, Tang Y, Shaikh M, Zhang LJ, Engen PA, Keshavarzian A (2007) Regulation of oxidant-induced intestinal permeability by metalloprotease-dependent epidermal growth factor receptor signaling. J Pharmacol Exp Ther 321:84–97. doi:10.1124/jpet.106.113019

Gomez-Mejiba SE, Zhai Z, Akram H, Deterding LJ, Hensley K, Smith N, Towner RA, Tomer KB, Mason RP, Ramirez DC (2009) Immuno-spin trapping of protein and DNA radicals: "tagging" free radicals to locate and understand the redox process. Free Radic Biol Med 46:853–865. doi:10.1016/j.freeradbiomed.2008.12.020

Gonzalez PK, Doctrow SR, Malfroy B, Fink MP (1997) Role of oxidant stress and iron delocalization in acidosis-induced intestinal epithelial hyperpermeability. Shock 8:108–114

Heron M, Hoyert DL, Murphy SL, Xu J, Kochanek KD, Tejada-Vera B (2009) Deaths: final data for 2006. Natl Vital Stat Rep 57:1–134

Huang YT, Ghio AJ, Nozik-Grayck E, Piantadosi CA (2001) Vascular release of nonheme iron in perfused rabbit lungs. Am J Physiol Lung Cell Mol Physiol 280:L474–L481

Iwatsuki H, Meguro R, Asano Y, Odagiri S, Li C, Shoumura K (2008) Chelatable Fe(II) is generated in the rat kidneys exposed to ischemia and reperfusion, and a divalent metal chelator, 2,2′-dipyridyl, attenuates the acute ischemia/reperfusion-injury of the kidneys: a histochemical study by the perfusion-Perls and -Turnbull methods. Arch Histol Cytol 71:101–114. doi:10.1679/aohc.71.101

Jordan JR, Moore EE, Sarin EL, Damle SS, Kashuk SB, Silliman CC, Banerjee A (2008) Arachidonic acid in post-shock mesenteric lymph induces pulmonary synthesis of leukotriene B4. J Appl Physiol 104:1161–1166. doi:10.1152/japplphysiol.00022.2007

Kozlov AV, Duvigneau JC, Hyatt TC, Raju R, Behling T, Hartl RT, Staniek K, Miller I, Gregor W, Redl H, Chaudry IH (2010) Effect of estrogen on mitochondrial function and intracellular stress markers in rat liver and kidney following trauma-hemorrhagic shock and prolonged hypotension. Mol Med. doi:10.2119/molmed.2009.00184

Lelli JL Jr, Pradhan S, Cobb LM (1993) Prevention of post-ischemic injury in immature intestine by deferoxamine. J Surg Res 54:34–38. doi:10.1006/jsre.1993.1006

Liaudet L, Soriano FG, Szabo E, Virag L, Mabley JG, Salzman AL, Szabo C (2000) Protection against hemorrhagic shock in mice genetically deficient in poly(ADP-ribose)polymerase. Proc Natl Acad Sci USA 97:10203–10208. doi:10.1073/pnas.170226797

Lillehei RC (1957) The intestinal factor in irreversible hemorrhagic shock. Surgery 42:1043–1054

Osband AJ, Deitch EA, Lu Q, Zaets S, Dayal S, Lukose B, Xu DZ (2003) The role of oxidant-mediated pathways in the cytotoxicity of endothelial cells exposed to mesenteric lymph from rats subjected to trauma-hemorrhagic shock. Shock 20:269–273. doi:10.1097/01.shk.0000079422.72656.66

Paller MS, Hedlund BE (1994) Extracellular iron chelators protect kidney cells from hypoxia/reoxygenation. Free Radic Biol Med 17:597–603

Penn AH, Hugli TE, Schmid-Schonbein GW (2007) Pancreatic enzymes generate cytotoxic mediators in the intestine. Shock 27:296–304. doi:10.1097/01.shk.0000235139.20775.7f

Puyana JC, Soller BR, Parikh B, Heard SO (2000) Directly measured tissue pH is an earlier indicator of splanchnic acidosis than tonometric parameters during hemorrhagic shock in swine. Crit Care Med 28:2557–2562

Rana MW, Shapiro MJ, Ali MA, Chang YJ, Taylor WH (2002) Deferoxamine and hespan complex as a resuscitative adjuvant in hemorrhagic shock rat model. Shock. 17:339–342

Rosario HS, Waldo SW, Becker SA, Schmid-Schonbein GW (2004) Pancreatic trypsin increases matrix metalloproteinase-9 accumulation and activation during acute intestinal ischemia-reperfusion in the rat. Am J Pathol 164:1707–1716

Rose S, Pizanis A, Silomon M (2000) Starch-deferoxamine conjugate inhibits hepatocyte Ca^{2+} uptake during hemorrhagic shock and resuscitation. J Trauma 49:291–296

Senthil M, Watkins A, Barlos D, Xu DZ, Lu Q, Abungu B, Caputo F, Feinman R, Deitch EA (2007) Intravenous injection of trauma-hemorrhagic shock mesenteric lymph causes lung injury that is dependent upon activation of the inducible nitric oxide synthase pathway. Ann Surg 246:822–830. doi:10.1097/SLA.0b013e3180caa3af

Singh B, Charkowicz D, Mascarenhas D (2004) Insulin-like growth factor-independent effects mediated by a C-terminal metal-binding domain of insulin-like growth factor binding protein-3. J Biol Chem 279:477–487. doi:10.1074/jbc.M307322200

Stahl GL, Xu Y, Hao L, Miller M, Buras JA, Fung M, Zhao H (2003) Role for the alternative complement pathway in ischemia/reperfusion injury. Am J Pathol 162:449–455

Stetler-Stevenson WG (2008) Tissue inhibitors of metalloproteinases in cell signaling: metalloproteinase-independent biological activities. Sci Signal 1:re6. doi:10.1126/scisignal.127re6

Stookey L (1970) Two new spectrophotometric reagents for copper. Talanta 17:644–647. doi:10.1016/0039-9140(70)80016-9

Thomas S, Balasubramanian KA (2004) Role of intestine in postsurgical complications: involvement of free radicals. Free Radic Biol Med 36:745–756. doi:10.1016/j.freeradbiomed.2003.11.027

Thomas DD, Espey MG, Vitek MP, Miranda KM, Wink DA (2002) Protein nitration is mediated by heme and free metals through Fenton-type chemistry: an alternative to the NO/O_2-reaction. Proc Natl Acad Sci USA 99:12691–12696. doi:10.1073/pnas.202312699

Turnage RH, Magee JC, Guice KS, Myers SI, Oldham KT (1994) Complement activation by the hydroxyl radical during intestinal reperfusion. Shock 2:445–450

Ulvik A, Kvale R, Wentzel-Larsen T, Flaatten H (2007) Multiple organ failure after trauma affects even long-term survival and functional status. Crit Care 11:R95. doi:10.1186/cc6111